

## Article

### Open Access

*J. Mex. Chem. Soc.* **2026**, 70(1):e2466

Received February 27<sup>th</sup>, 2025

Accepted February 9<sup>th</sup>, 2026

<http://dx.doi.org/10.29356/jmcs.v70i1.2466>  
e-location ID: 2466

#### Keywords:

Ozonation, pharmaceutical degradation, wastewater treatment, ambroxol, dextromethorphan

#### Palabras clave:

Ozonación, degradación de fármacos, tratamiento de aguas residuales, ambroxol, dextrometorfano

#### \*Corresponding author:

Arizbeth Pérez-Martínez

email:

[arizbeth.perez@lasalle.mx](mailto:arizbeth.perez@lasalle.mx)

©2026, edited and distributed by Sociedad  
Química de México

ISSN-e 2594-0317

## Degradation of Histiacyl NF® in Wastewater by Simple Ozonation: Kinetics and byproduct Formation

Diana Calderón Suárez<sup>1</sup>, Elizabeth Reyes<sup>1</sup>, Arizbeth Pérez-Martínez<sup>2\*</sup>, Isaac Chairez<sup>3</sup>

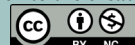
<sup>1</sup>Facultad de Ciencias Químicas, Universidad La Salle México, Benjamín Franklin No 45 Alcaldía Cuauhtémoc, Ciudad de México, México, 06140.

<sup>2</sup>Vicerrectoría de Investigación, Universidad La Salle México, Benjamín Franklin No 45 Alcaldía Cuauhtémoc, Ciudad de México, México, 06140.

<sup>3</sup>Institute of Advanced Materials for the Sustainable Manufacturing, Tecnológico de Monterrey, Jalisco México, 45210.

**Abstract.** Ozonation is wastewater treatment use for the degradation of recalcitrant pollutants such as pharmaceutical compounds; however, the kinetic characterization and transformation pathway analysis remain partial for complex medicinal mixtures. The ozonation of commercial pharmaceutical formulation containing ambroxol and dextromethorphan (Histiacyl® NF) was analyzed at laboratory scale under controlled semi-continuous operational conditions. The wastewater treatment efficiency was evaluated through UV-Vis spectroscopy, BOD<sub>5</sub> variation, electrical conductivity measurements, and HPLC analysis for identification and quantification of final reaction products. Ozonation achieved up to a 95 % decomposition of Histiacyl® NF within 15 minutes, as demonstrated by UV-Vis absorbance decline at characteristic wavelengths and confirmed by HPLC analysis. The progressive increase in BOD<sub>5</sub> and electrical conductivity indicated the conversion of the initial molecules of ambroxol and dextromethorphan into smaller, more polar, and potentially biodegradable species. Oxalic acid was identified and quantified as the main accumulated final product by HPLC analysis, which concentration obtained was consistent with stoichiometric predictions. A kinetic model based on pseudo-first-order was established to define both the decomposition of

©2026, Sociedad Química de México. Authors published within this journal retain copyright and grant the journal right of first publication with the work simultaneously licensed under a [Creative Commons Attribution License](#) that enables reusers to distribute, remix, adapt, and build upon the material in any medium or format for noncommercial purposes only, and only so long as attribution is given to the creator.



dextromethorphan and the formation and consumption of oxalic acid.

The results demonstrate that ozonation is an effective and reproducible treatment strategy for complex pharmaceutical mixtures and highlight the relevance of kinetic modeling as a predictive tool for process optimization and scale-up in water and wastewater treatment applications.

**Resumen.** El proceso de ozonación es ampliamente utilizado en la degradación de contaminantes recalcitrantes como los compuestos farmacéuticos; sin embargo, la caracterización de la cinética de reacción y el análisis de las rutas de transformación siguen siendo parciales para mezclas farmacéuticas complejas. En el presente trabajo se analizó a escala de laboratorio la ozonación de una formulación comercial que contiene ambroxol y dextrometorfano (Histiacil NF) bajo condiciones operativas controladas.

La eficiencia del tratamiento de degradación se evaluó mediante Espectroscopía UV-Vis, variación de DBO<sub>5</sub>, Conductividad Eléctrica y el análisis por HPLC para la identificación y cuantificación de los productos finales de reacción. Mediante este proceso se alcanzó un 95 % de descomposición de Histiacil® NF en 15 minutos, demostrado en la disminución de la absorbancia UV-Vis en longitudes de onda, el incremento progresivo de la DBO<sub>5</sub> y la conductividad eléctrica, lo cual indica la conversión de las moléculas iniciales de ambroxol y dextrometorfano en especies más pequeñas, más polares y potencialmente biodegradables.

El ácido oxálico fue identificado y cuantificado como el principal producto final acumulado mediante análisis por HPLC. Se estableció un modelo cinético basado en pseudo-primer orden para definir tanto la descomposición del dextrometorfano como la formación y consumo del ácido oxálico.

Los resultados demuestran que la ozonación es una estrategia de tratamiento efectiva y reproducible para mezclas farmacéuticas complejas, destacando la relevancia del modelado cinético como una herramienta predictiva para la optimización y escalamiento del proceso en aplicaciones de tratamiento de agua y aguas residuales.

## Introduction

Global economic growth metrics have been significantly impacted by the unregulated expansion of anthropogenic activities, including chemical and processing industry, agricultural chemistry, urbanization, among others [1]. This phenomenon has driven an increase in consumer demand and rising standards, which, in turn, have exacerbated environmental pollution issues. Furthermore, large quantities of chemicals and trace elements caused by the improper disposal of waste, industrial discharges, spills, and soil contamination have infiltrated our water bodies [2].

There has been a surge in studies examining the presence of a new category of substances in water environments, collectively referred to as "emerging contaminants." These substances encompass a wide range of compounds widely used around the world, such as agrochemical products, cosmetics, personal hygiene products, and pharmaceuticals, among others [2,3]. Most notably, many recently synthesized compounds—suspected of causing harm even at minimal concentrations—tend to combine with other compounds or be released into the ecosystem as degradation byproducts. This concerning list includes pharmaceutical wastes, microplastics, endocrine disruptors, hormones, and several chemicals' compounds. Their widespread dissemination in ecosystems is mainly due to improper disposal of municipal, domestic, and industrial wastewater [4].

An example of this type of emerging compounds is Ambroxol, an expectorant medication commonly utilized to enhance surfactant release in the lungs and reduce mucus viscosity; however, Ambroxol presents a persistent environmental challenge [5], with presence in untreated wastewater effluents, and surface water bodies, with pollutant concentrations from 4.9 to 1047 ng L<sup>-1</sup>, respectively [6]. Unfortunately, Ambroxol exhibits limited degradability in municipal wastewater treatment plants, compromising the operational efficiency of biological wastewater treatment process [6-10].

Another concerning medical compound is Dextromethorphan, a widely used antitussive drug often combined with Ambroxol. Both Dextromethorphan and Ambroxol have high water solubility, making them more likely to be found in water and wastewater [11,12].

To protect our environment, it is imperative to improve water treatment technologies that reduce the pharmaceutical residues through wastewater effluents. Ozonation stands out as one of the most effective

wastewater treatment methodologies due to its ability to oxidize organic contaminants using molecular ozone ( $\text{pH} \leq 6$ ) or hydroxyl radicals ( $\text{pH} \geq 7$ ). Ozonation process has been proved to be effective as a final treatment for wastewater containing antibiotics and various pharmaceuticals [4, 13-16] as is shown in Table 1.

**Table 1.** Recent contributions to pharmaceutical degradation by Ozonation.

Reference	Contaminant conditions	Ozonation conditions	Main results
(Zheng, 2024) [17]	Oseltamivir Phosphate (OP, 1.0 $\mu\text{M}$ )	Volume 20 mL	90 % OP removal with 10 and 20 $\mu\text{M}$ in 30 and 16 seconds. In wastewater effluents, efficiency decreases due to organic matter, requiring an ozone dose of 0.544 $\text{g}_{\text{O}_3}/\text{g}_{\text{DOC}}$ to achieve 95 % OP degradation.
(Adamek, 2024) [18]	Sodium ampicillin salt, AMP, 0.27 mmol/L Doxycycline hyclate, DOX, 0.10 mmol/L Tylosin tartrate, TYL, 0.19 mmol/L Sodium sulfathiazole salt, STZ, 1.0 mmol/L Volume 350 mL	Ozone concentration 15 g/h Gas flow rate 0.8 L/min (15 % V/V $\text{O}_3$ )	Ozonation effectively degraded the studied antibiotics; however, mineralization was not achieved. The main products obtained showed lower ecotoxicity compared to the original antibiotic molecules.
(Beltran, 2024) [19]	Metronidazole, 5 mg/L Volume 0.5 L	Initial pH 5.8 Flow rate 10 L/h Ozone concentration 5 mg/L	Direct photolysis removed approximately 70 % of Metronidazole in 120 minutes. Ozonation combined with radiation achieved total removal in 45 minutes, showing a synergistic effect between ozone and UV radiation.
(Prada-Vásquez, 2024) [20]	Wastewater effluents collected from the Mediterranean coast of Spain. TOC: 49.61, 67.3 mg/L DOC: 47.5, 65.4 mg/L TIC: 1.13, 20.3 mg/L	Zeolites Y: NaY 60, NaY 12 Gas flow rate 2.0 L/min Ozone concentration: 6.1 $\text{gNm}^{-3}$ pH 1.71.7	Catalytic ozonation with NaY-12 zeolite removed 95 % of a mixture of 25 pharmaceutical compounds identified in wastewater effluents in 9 minutes. Using NaY-60 zeolite achieved the same removal in 12 minutes. In comparison, direct ozonation removed 95 % in 25 minutes.
(Aseman-Bahiz, 2024) [21]	Aspirin in concentrations of 5.0 – 50 mg/L	Ozone flow rate, 200 mg/h Ozone dose, 50, 80, 100, 140, and 170 mg/L; Nano- $\text{FeS}_2$ solution; Reactor volume 250 mL, equipped with stainless steel electrodes and an ultrasonic homogenizer with an output power of 200 W and a frequency of 26 kHz. Total reaction time 30 minutes.	In the nano- $\text{FeS}_2$ /PMS system, 99.2 % aspirin removal was achieved in 30 minutes, with an 81.6 % reduction in TOC. In the nano- $\text{FeS}_2/\text{O}_3$ system, 98.6 % aspirin removal was achieved, with a 77.4 % reduction in TOC.

In this study, the degradation of the pharmaceutical mixture ambroxol/dextromethorphan (Histiacyl®) was carried out by simple ozonation. The decomposition efficiency was corroborated by HPLC analysis, BOD<sub>5</sub> measurements, ozone consumption and reaction kinetics determination by the implementation of a mathematical model.

## Materials and methods

### Preparation of the Histiacyl® NF Solution

A solution of commercial Histiacyl® NF (Sanofi-Aventis de México S.A. de C.V.) was prepared with distilled water. The concentration of 0.125 ppm was selected as it provided adequate signal intensity and reproducibility while remaining within the linear response range and sensitivity limits of both UV–Vis spectrophotometry and HPLC analyses. This concentration allowed reliable monitoring of absorbance changes and chromatographic detection throughout the ozonation process without signal saturation or excessive noise. The physicochemical characteristics of the solution at the beginning of the ozonation process are presented in Table 2. The pH value and Electrical Conductivity were determined using a Thermo Scientific™ Orion Star™ A211. Data are presented as the mean of triplicate determinations.

**Table 2.** Histiacyl® NF physicochemical specifications.

Variable	Concentration	pH	Electrical Conductivity	Commercial Ratio
Value	0.125 ppm	4±0.1	119.7 $\mu\text{S}/\text{cm}^2 \pm 0.5$	Dextromethorphan ( $\text{C}_{18}\text{H}_{25}\text{NO}$ ) / Ambroxol ( $\text{C}_{13}\text{H}_{18}\text{N}_2\text{Br}_2\text{O}$ ) (250 mg:250 mg)

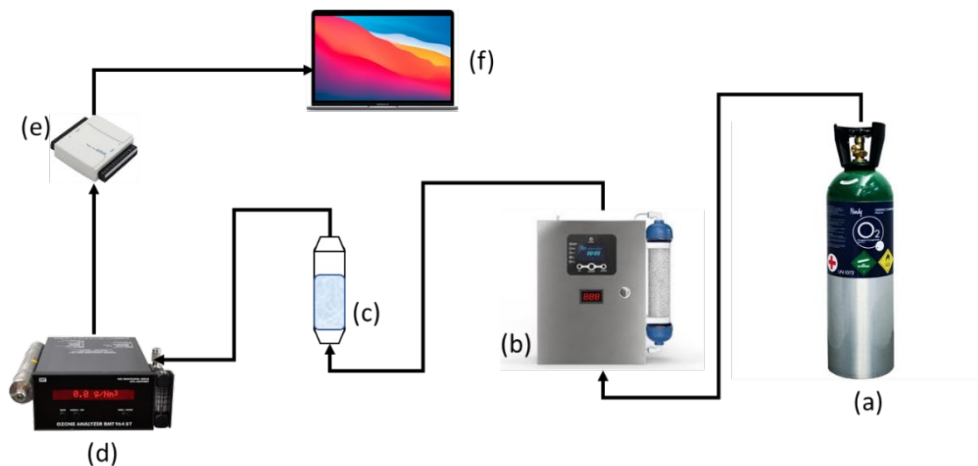
### Ozonation process at laboratory level

Fig. 1 illustrates the laboratory-scale ozonation system used in all experiments, which were conducted at  $25 \pm 3$  °C. As shown in Fig. 1(a), oxygen was supplied from a pressurized oxygen tank and fed at a gas flow rate of  $0.25 \text{ L min}^{-1}$  into a corona discharge ozone generator (Fig. 1(b)), model HTU500G (AZCO Industries Limited, Langley, British Columbia, Canada), where ozone was generated at an initial gas-phase concentration of  $35 \text{ mg L}^{-1}$ .

The generated gaseous mixture of ozone–oxygen was introduced into a semi-batch glass reactor with a working volume of 250 mL (Fig. 1(c)). To ensure homogeneous gas distribution and efficient mass transfer, a porous glass diffuser was installed at the bottom of the reactor.

The ozone concentration in the inlet and outlet streams was monitored using a BMT-930 analyzer (Fig. 1(d)); data were captured via a DA-card (Fig. 1(e)) and processed on a PC (Fig. 1(f)). A data acquisition software recorded the temporal variation of ozone concentration in gas phase versus reaction time, commonly referred to as ozonograms. These data were subsequently used to evaluate ozone consumption and to determine the reaction kinetics in the ozonation process.

Liquid samples were withdrawn from the reactor at predefined reaction times (0.0, 5.0, 7.5, and 15 min) for analytical characterization of Histiacyl® NF degradation and the identification and quantification of transformation products formed throughout the ozonation process.



**Fig. 1.** Scheme of Ozonation process at laboratory level: (a) extra dry oxygen tank, (b) corona discharge ozone generator, (c) 250 mL Glass reactor, (d) ozone gas-phase sensor, (e) data acquisition card, (f) computer.

### Analytical methods

The studies to characterize the decomposition efficiency of Histiacyl® NF included UV-Vis spectrophotometric analysis and BOD<sub>5</sub> measurements. Initially, a full wavelength scan of the solution was performed in the UV-Vis range to identify the characteristic absorption bands of the medicinal mixture. Based on this spectral scan, the characteristic wavelength selected was 410 nm, as shown in Fig. 2, and the decomposition process was monitored by measuring absorbance variations within this range. Additionally, BOD<sub>5</sub> was determined using a BOD<sub>5</sub> detector (Model 890, Standard Method 5210D) with Hach BODTrak™ II and Hach reagents.

HPLC analysis was performed using a YL9100 system (YL Instruments) equipped with a UV detector to determine the variation of initial and final accumulated reaction compounds. Detection was carried out at a wavelength of 210 nm [22,23]. The HPLC conditions were selected based on previously reported methods for the determination of ambroxol, dextromethorphan, and structurally related pharmaceutical compounds, as well as preliminary optimization assays conducted in this study [1-3]. An HPLC column Agilent Eclipse XDB-C18 (4.6 × 150 mm) in reversed-phase was selected due to its proven suitability for the separation of moderate polar pharmaceutical compounds and its widespread application in pharmaceutical and environmental analyses [1,2].

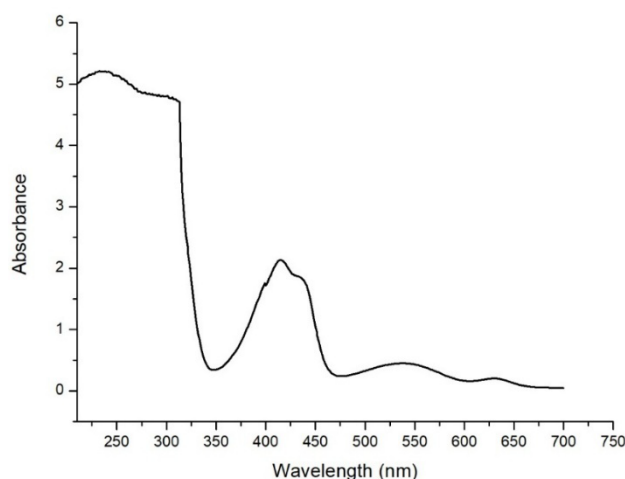


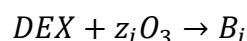
**Fig. 2.** The UV-Vis spectrum of Histiacyl NF® showed the characteristic wavelength of 410 nm.

The HPLC mobile phase consisted of a mixture of phosphate buffer (pH 4) and acetonitrile (9:1, v/v) with a flow rate of 1.1 mL·min<sup>-1</sup>. These parameters were selected to favor the protonated form of the target compounds, improving retention and reproducibility and optimized the resolution and analysis time [1-3]. All analyses were carried out at 25 °C ± 3.0 using degassed solvents (acetonitrile and sodium phosphate, JT Baker).

### Kinetic analysis

Mathematical modeling of the ozonation process has become an important tool for enhancing the understanding of ozonation process as water treatment method. In general terms, modeling the ozonation of Histiacyl® NF is complicated by the intricate network of series and parallel reactions that characterize the degradation process.

In this study, the commercial mixture of dextromethorphan/ambroxol (DEX) was considered the target contaminant present at the beginning of the ozonation. The interaction between ozone molecules and DEX was assumed to follow an irreversible second-order reaction, dependent on both the DEX concentration and the dissolved ozone concentration. The overall reaction scheme can be presented as:



where  $B_i$  represents each one of the byproducts obtained from the reaction between the ozone and the DEX, and the coefficient  $z_i$  represents the stoichiometric coefficient relating ozone molecules to DEX consumption. Under this assumption, the rate of DEX degradation is expressed as Equation (1):

$$-r_D = k_{DEX} C_{DEX} C_{O_3} \quad (1)$$

where  $r_D$  is the reaction rate of DEX decomposition (mg·L<sup>-1</sup>·min<sup>-1</sup>),  $k_{DEX}$  is the second-order reaction rate constant (L·mg<sup>-1</sup>·min<sup>-1</sup>),  $C_{DEX}$  is the DEX concentration in the liquid phase (mg·L<sup>-1</sup>), and  $C_{O_3}$  is the ozone concentration in the liquid phase (mg·L<sup>-1</sup>).

Because the experiments were conducted in a semi-batch reactor, no initial influent concentration of DEX exists. The following mass balance relationships apply:

$$C_{DEX} = -C_{DEX,r} \quad (2)$$

$$C_{O_3} = C_{O_3,in} - C_{O_3,r} - C_{O_3,out} \quad (3)$$

$$C_{O_3,r} = z C_{DEX,r} \quad (4)$$

where  $C_{DEX,r}$  is the amount of DEX reacted,  $C_{O_3,in}$  is the ozone concentration at the reactor inlet,  $C_{O_3,r}$  is the ozone concentration consumed over a given time due to the reaction with DEX, and  $C_{O_3,out}$  correspond to the ozone concentration at the reactor outlet in gas phase, which is influenced by mass transfer between the liquid phase and the reactor headspace.

Combining Equations (3) and (4), the ozone concentration in the liquid phase can be expressed as:

$$C_{O_3} = m_{DEX} - C_{O_3,out} \quad (5)$$

where  $m_{DEX}$  is defined as:

$$m_{DEX} = C_{O_3,in} - z C_{DEX,r}$$

And represents the effective ozone concentration available for reaction with DEX and its transformation products.

Assuming an excess of ozone in the reactor, the kinetic behavior of DEX degradation can be described using a pseudo-first-order approximation with respect to DEX concentration. Under this assumption, the kinetic model governing DEX degradation is given by Equation (6):

$$\frac{dC_{DEX}(t)}{dt} = -k_{DEX}C_{DEX}(t)C_{O_3}(t) \quad (6)$$

where  $C_{DEX}(t)$  and  $C_{O_3}(t)$  represents the time-dependent concentration of DEX and ozone, respectively.

For final byproducts such as oxalic acid (OA), it was assumed that they are directly formed from the decomposition of DEX. The accumulation and degradation of OA during ozonation were modeled as follows:

$$\frac{dC_{OA}(t)}{dt} = k_{OA,DEX}C_{DEX}(t) - k_{OA}C_{OA}(t)C_{O_3}(t) \quad C_{OA}(0) = C_{OA,0} \quad (7)$$

where  $k_{OA,DEX}$  is the reaction rate constant associated with OA formation from DEX,  $k_{OA}$  is the reaction rate constant for OA degradation, and  $C_{OA}(t)$  is the OA concentration time (t).

The estimation of the kinetic parameters  $k_{DEX}$ ,  $k_{OA,DEX}$ , and  $k_{OA}$ , was carried out using an exact robust differentiator, as reported in [24], which provides numerical approximations of the time derivatives of experimentally measured concentration profiles. The output of the differentiation is denoted as  $y(t)$ , leading to the expression shown in Equation (8):

$$y(t) = k_{OA,DEX}C_{DEX}(t) - k_{OA}C_{OA}(t)C_{O_3}(t) + \varepsilon(t) \quad (8)$$

where  $y(t)$  is the estimate of the temporal derivative of the analyzed variable, and  $\varepsilon(t)$  represents the approximation error introduced by the differentiator process.

Due to the fact that  $C_{DEX}(t)$  and  $O_3(t)$  were obtained at different sampling times, a third – order polynomial interpolation of the ozonogram data was applied to generate synchronized datasets with uniform time intervals. This allowed the parametric identification problem to be expressed in the discrete form shown in Equation (9):

$$y(t_k) = \theta^T \varphi \left( C_{DEX}(t_k), C_{O_3}(t_k) \right) + \varepsilon(t_k) \quad (9)$$

where  $\theta$  is the vector of unknown kinetic parameters,  $\varphi$  is the regression vector composed of the measured concentrations,  $t_k$  represents the discrete sampling time ( $k= 1, 2, \dots, k$ ), and the superscript T denotes the transpose of the parameter vector.

Finally, the least-squares solution for parameter estimation is given by Equation (10):

$$\theta^* = \sum_{k=1}^K \left( \varphi^T \left( C_{DEX}(t_k), C_{O_3}(t_k) \right) \varphi \left( C_{DEX}(t_k), C_{O_3}(t_k) \right) \right)^{-1} \sum_{k=1}^K \left( \varphi \left( C_{DEX}(t_k), C_{O_3}(t_k) \right) y(t_k) \right) \quad (10)$$

## Results and discussion

### Ozone consumption during the reaction and determination of reaction kinetics

The decomposition of ozone in aqueous solution is significantly influenced by pH, especially in an acidic environment, where ozone decomposition is characterized by a slower reaction rate compared to neutral or alkaline conditions. Fig. 3 shows ozone consumption during the ozonation process; this graph, known as an ozonogram, provides indirect information on the reaction behavior between the pharmaceutical compound and ozone, as stated by Poznyak and García, 2008 [25].

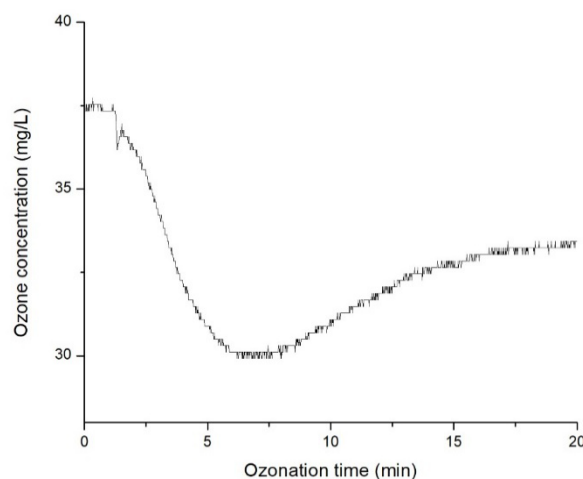
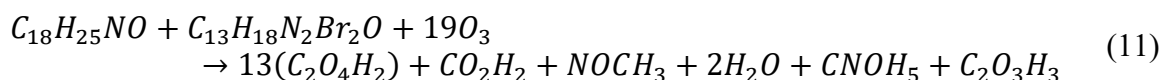


**Fig. 3.** Ozonogram of Histiacyl® NF through 20 minutes of reaction.

Upon initiation of the oxidation process, a decrease in ozone concentration in gas phase was observed, resulting from the saturation of the reactor and subsequent interaction with the Histiacyl® NF (ambroxol/dextromethorphan) compounds. The ozone in aqueous phase reaches its lowest point before rising again once the contaminant is completely degraded, eventually returning to the initial ozone concentration value. According to [21], kinetic insights are provided indirectly by the ozonogram, as variations in the gradient correspond to critical phases of the oxidation process. In this study, such fluctuations delineate the degradation of Histiacyl® NF, the evolution of intermediate species, and the eventual formation of stable end-products like oxalic acid, which exhibit minimal reactivity toward ozone [26].

The stoichiometric reaction of ozone with Histiacyl® NF is presented below, where oxalic acid is the main product formed:



Following the proposed strategy, the estimated reaction rate constants for DEX under conventional ozonation were determined as:  $k_{DEX} = 0.8 * 10^{-4} \frac{L}{mol*s}$ ,  $k_{OA,DEX} = 1.4 * 10^2 \frac{L}{mol*s}$  y  $k_{OA} = 0.2 * 10^{-7} \frac{L}{mol*s}$ . The marked discrepancy between  $k_{DEX}$  and  $k_{OA,DEX}$  suggests that DEX degradation proceeds through several unidentified intermediates. These species undergo continuous ozonation, ultimately yielding oxalic acid as a persistent byproduct.

### Decomposition dynamics

Fig. 4 presents the decomposition dynamics of Histiacyl® NF monitored by UV-Vis spectroscopy at 410 nm, while Table 3 summarizes the variation of BOD<sub>5</sub> and electrical conductivity after 20 minutes of ozonation. The UV-Vis results show that after 15 minutes of reaction, approximately 95 % degradation of Histiacyl® NF was achieved, as evidenced by the substantial decrease in absorbance intensity. This high removal efficiency confirms the effectiveness of ozonation for the rapid oxidation of the Histiacyl® NF.

Simultaneously, the observed increase in BOD<sub>5</sub> values and changes in electrical conductivity indicate the formation of more biodegradable and oxidized transformation products, consistent with partial mineralization and the accumulation of low-molecular-weight organic acids [17-19]. The combined analysis of UV-Vis degradation, BOD<sub>5</sub> enhancement, and conductivity variation demonstrates a strong correlation between ozonation efficiency and the generation of intermediates suitable for subsequent biological treatment,

supporting the potential integration of ozonation as a pretreatment step in a coupled process of advanced oxidation–biological treatment [27,28].

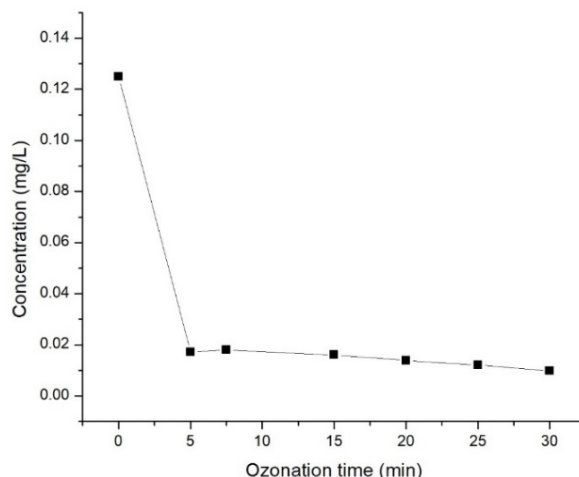


**Fig. 4.** Decomposition Dynamics of Histiacyl® NF.

**Table 3.** Variation of BOD<sub>5</sub>, pH, and electrical conductivity before and after the ozonation process.

Variable	Initial Value	Final Value
pH	4	4
Electrical Conductivity ( $\mu\text{S}/\text{cm}^2$ )	119.7	149.2
BOD 5	200	22

Electrical conductivity increased by nearly 20 % post-treatment; a trend attributable to the generation of ions during the ozone-induced breakdown of Histiacyl® NF, which leads to the release of inorganic ions and protonated functional groups, including bromide ions originating from dextromethorphan hydrobromide and nitrogen-containing species derived from tertiary and secondary amine oxidation. This parameter is therefore relevant as it supports the observed enhancement in biodegradability and the formation of low-molecular-weight, water-soluble species suitable for subsequent biological treatment.

#### Identification of final compounds

This study identified oxalic acid as the main final compound during the ozonation process, as shown in Fig. 5. The identification and quantification of oxalic acid were carried out by HPLC using the analytical conditions described in Section 2.3. Compound identification was based on retention time comparison with an oxalic acid standard, while quantification was achieved through an external calibration curve constructed from standard oxalic acid solutions at known concentrations. The results indicate that oxalic acid reached its maximum concentration at 5 minutes of reaction and then remained approximately constant throughout the reaction time ( $237 \text{ mg L}^{-1}$ ). This value is consistent with the stoichiometrically calculated concentration of  $240 \text{ mg L}^{-1}$  [29].

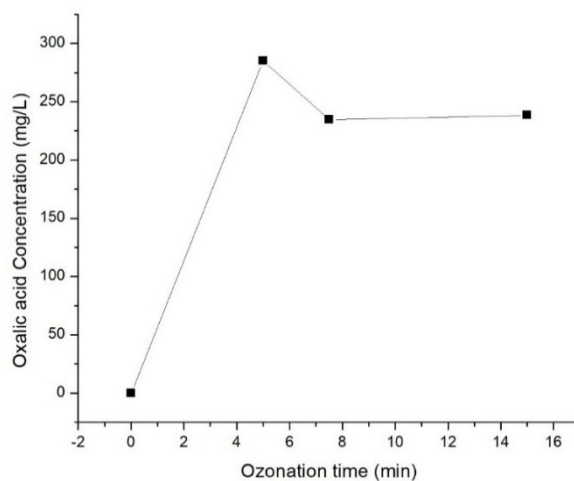


Fig. 5. Oxalic acid concentration during the ozonation process.

## Conclusions

This study demonstrates the feasibility and effectiveness of ozonation process for the treatment of pharmaceutical mixtures containing ambroxol and dextromethorphan. The process efficiency was validated through analytical techniques, including UV-Vis spectroscopy, BOD<sub>5</sub> evolution, electrical conductivity variation, and HPLC analysis, upholding the validity and steadfastness of the results obtained.

The high degradation efficiency observed, reaching 95 % within short reaction times, confirms the strong oxidative capacity of ozone toward complex medicinal formulations. The simultaneous increase in BOD<sub>5</sub> and electrical conductivity provides evidence of molecular fragmentation and transformation of recalcitrant parent compounds into smaller, more polar, and potentially biodegradable species. These results suggest that ozonation not only removes pharmaceutical contaminants but also enhances the suitability of the treated effluent for subsequent biological processes.

A key contribution of this work is the development and application of a kinetic modeling framework based on pseudo-first-order reactions. This approach allowed the quantitative description of both contaminant degradation and byproduct accumulation, providing insight into ozone consumption, reaction stages, and rate-limiting steps.

Overall, the combined experimental and modeling approach presented in this study strengthens the understanding of ozonation mechanisms for pharmaceutical mixtures and supports its application as a reliable treatment technology in water and wastewater treatment systems.

## Acknowledgements

Conceptualization, A.P.M, Methodology, D.C.S, E.R. and A.P.M.; Software, I.C.; Validation, I.C. and A.P.M.; Formal analysis, I.C.; Investigation, D.C.S. and A.P.M.; Resources, A.P.M.; Data curation, I.C.; Writing-original draft preparation, D.C.S. and I.C.; Writing – review and editing, A.P.M.; Supervision, A.P.M., Project administration, A.P.M.; Funding acquisition, A.P.M.

## References

1. Giudice, L.; Llamas-Clark, E.; DeNicola, N.; Pandipati, S.; Zlatnik, M.; Decena, D.; Woodruff, T.; Conry, J. *Int. J. Gynecol. Obstet.* **2021**, *155*, 345-356.
2. Galindo-Miranda, J.; Guízar-González, C.; Becerril-Bravo, E.; Moeller-Chávez, G.; León-Becerril, E.; Vallejo-Rodríguez, R. *Water Supply.* **2019**, *19*, 1871-1884.
3. Lahiri, A.; Daniel, S.; Kanthapazham, R.; Vanaraj, R.; Thambidurai, A.; Peter, L. *J. Hazard. Mater. Adv.* **2023**, 100266.
4. Huber, M.; Göbel, A.; Joss, A. H. A.; Löffler, D.; McArdell, C.; Ried, A.; Siegrist, H.; Ternes, T.; von Gunten, U. *Environ. Sci. Technol.* **2005**, *39*, 4290-4299.
5. Brüggemann, H.; Köser, H.; Meyer, E.; Nguyen, T.-H. *Water Res.* **2003**, *37*, 674-680.
6. Wang, L.; Xu, H.; Lu, J.; Chovelon, J.-M.; Ji, Y. *Water Res.* **2022**, 119275.
7. Xu, J.; Ma, Y.; Wei, J.; Li, F.; Peng, X. *Chem. Pap.* **2015**, *69*, 722-728.
8. Zhang, Y.; Lei, D.; Wang, B.; Liu, C.; Jia, Y.; Zhai, N.; Blaney, L.; Yu, G. *Environ. Pollut.* **2020**, 114113.
9. Brown, A.; Ackerman, J.; Cicek, N.; Wong, C. *Environ. Pollut.* **2000**, 114852.
10. Zhi, H.; Miannecki, A.; Kolpin, D.; Klaper, R.; Iwanowicz, L.; LeFevre, G. *Water Res.* **2021**, 117537.
11. Mani, N.; Jun, H.; Beach, J.; Nerurkar, J. *Pharm. Dev. Technol.* **2003**, *8*, 385-396.
12. Mostafa, H.; Ibrahim, M.; Sakr, A. *Pharm. Dev. Technol.* **2013**, *18*, 454-463.
13. Androozzi, R.; Canterino, M.; Marotta, R.; Paxeus, R. *J. Hazard. Mater.* **2005**, *122*, 243-250.
14. Dantas, R.; Contreras, S.; Sans, C.; Esplugas, S. *J. Hazard. Mater.* **2008**, *150*, 790-794.
15. Rosal, R.; Rodríguez, A.; Perdigón-Melón, J.; Petre, A.; García-Calvo, E.; Gómez, M. J.; Agüera, A.; Fernández-Alba, A. *Water Res.* **2010**, *44*, 578-588.
16. Fedorova, G.; Grabic, R.; Nyhlén, J.; Järhult, J. D.; Söderström, H. *Chemosphere.* **2015**, *134*, 1-8.
17. Zheng, M.; van Beek, S. J.; Sánchez-Montes, I.; Xu, B.; Gamal El-Din, M. *J. Environ. Chem. Eng.* **2024**, 114297.
18. Adamek, E.; Baran, W. *J. Hazard. Mater.* **2024**, 134026.
19. Beltrán, F.; Jiménez-López, M.; Álvarez, P.; Rivas, F. *J. Ind. Eng. Chem.* **2024**.
20. Prada-Vásquez, M. A.; Simarro-Gimeno, C.; Vidal-Barreiro, I.; Cardona-Gallo, S. A.; Pitarch, E.; Hernández, F.; Torres-Palma, R. A.; Chica, A.; Navarro-Laboulais, J. *Sci. Total Environ.* **2024**, 171625.
21. Aseman-Bahiz, E.; Sayyaf, H. *J. Contam. Hydrol.* **2024**, 104419.
22. Ternes, T. A. *TrAC Trends Anal. Chem.* **2021**, *20*, 419-434.
23. Ferrer, I.; Thurman, E. M. *TrAC Trends Anal. Chem.* **2003**, *22*, 750-756.
24. Cruz-Zavala, E.; Moreno, J. A.; Fridman, L. M. *IFAC Proc. Vol.* **2011**, *44*, 3039-3044.
25. Poznyak, T.; García, A. *Ozonoterapia.* **2008**, 15-23.
26. Razumovskii, S. *Chem. Kinet.* **2005**, 259.
27. von Gunten, U. *Water Res.* **2003**, *37*, 1443-1467.
28. Lee, Y.; von Gunten, U. *Water Res.* **2010**, *44*, 555-566.
29. Tab, A.; Dahmane, M.; Belabed, C.; Bellal, B.; Richard, C.; Trari, M. *Sci. Total Environ.* **2021**, 146451.